cell stress

Research Article

www.cell-stress.com

Neuroglobin-enriched secretome provides neuroprotection against hydrogen peroxide and mitochondrial toxin-induced cellular stress

Giovanna Bastari[1,a], Virginia Solar Fernandez[1,2,a], Maurizio Muzzi[3,4], Sandra Moreno[3,5], Maria Marino[1,5,*] and Marco Fiocchetti[1,5,*]

[1]Department of Science, Section Biomedical Sciences and Technology, University Roma Tre, V.le G. Marconi, 446, 00146, Rome, Italy. [2]Present address: Instituto de Investigaciones Biomédicas "Alberto Sols" UAM-CSIC, Arturo Duperier, 4, 28029 Madrid, Spain; Department of Biochemistry, School of Medicine, Universidad Autonóma de Madrid, 28029 Madrid, Spain. [3]Department of Science, Section Molecular, Cellular, Environmental and Evolutionary Biology, LIME, University Roma Tre, V.le G. Marconi, 446, 00146, Rome, Italy. [4]Department of Bioscience and Territory, University of Molise, Contrada Fonte Lappone, 86090, Pesche, Italy. [5]IRCCS Fondazione Santa Lucia, via del Fosso di Fiorano, 64, 00179, Rome, Italy

*Corresponding Authors:
Maria Marino; E-mail: maria.marino@uniroma3.it
Marco Fiocchetti, Tel.: 0039 06 5733 6455; E-mail: marco.fiocchetti@uniroma3.it

[a]Equal contribution as a first author.

ABSTRACT Aberrant response to physiological cell stress is part of the mechanisms underlying the development of diverse human diseases, including neuropathologies. Neuroglobin (NGB), an intracellular monomeric globin, has gained attention for its role in endogenous stress response pathways in neuroprotection. To date, evidence supports the concept of NGB as an inducible protein, triggered by physiological and pathological stimuli via transcriptional and/or post-transcriptional mechanisms, offering cell-autonomous neuroprotective functions under various cellular stresses. Notably, recent evidence suggests the extracellular occurrence of NGB. We aimed to explore whether NGB redistribution in the cell microenvironment may serve in transmitting resilience capability in a model with neuronal characteristics. Results obtained in SH-SY5Y demonstrated that intracellular NGB upregulation is associated with the promotion of the extracellular release of the globin. Additionally, cell secretome from NGB-overexpressing cells, characterized by globin accumulation, exhibits protective effects against oxidative stress and mitochondrial toxicity, as evidenced by reduced apoptosis and preserved mitochondrial structure. These findings shed light on the potential significance of extracellular NGB as part of a common cell response to physiological and stress conditions and as a factor promoting cell resilience. Furthermore, the potential for neuroprotection of extracellular NGB paves the way for future therapeutic opportunities.

doi: 10.15698/cst2024.11.300
Received originally: 09. 02. 2024;
in revised form: 30. 09. 2024,
Accepted: 30. 10. 2024
Published: 20. 11. 2024

Keywords: neuroglobin, secretome, neuronal stress, neurodegeneration, mitochondria

Abbreviations:
3-NP - 3-nitropropionic acid,
CM - conditioned medium,
EV - extracellular vesicle,
NGB - neuroglobin,
sEV - small EV,
WT - wild type

INTRODUCTION

Cellular response to stress relies on evolutionary conserved mechanisms aimed at maintaining homeostasis and facilitating adaptation to new cellular environments [1]. Under stressful conditions, post-mitotic neurons are hardly replaced. Rather, mature neurons exhibit two prominent features: (i) the utilization of anti-apoptotic mechanisms [2]; and (ii) the activation of powerful stress response pathways, aimed at mitigating the effects of both intrinsic and extrinsic insults [3].

In the scenario of searching for novel neuroprotective mechanisms to strengthen neuronal resilience, in the past two decades, the discovery of neuroglobin (NGB) [4] has unveiled a potential new avenue for therapeutic interventions in various neuropathologies. Accumulating evidence has revealed a function of NGB as an endogenous cellular protectant, emphasized by its preferential expression in neurons [5–7], although the presence of the globin has been also reported in astrocyte [8, 9], retinal glial cells [10] and microglial cells [11, 12], especially in response to stress condition. A plethora of *in vitro* and *in vivo* studies have demonstrated the role of overexpressed or ectopic expression of the globin in preserving neuronal function and viability under stress conditions including, but not limited to, oxidative stress [13–16], hypoxic/ischemic injuries [17–19],

neuroinflammation [20] and neurodegeneration [5, 6, 16, 21–23].

The idea that the NGB upregulation serves as a physiological acute protective response, prompted researchers to identify modulators of endogenous globin. Our group showed that the 17β-estradiol (E2)/estrogen receptor β (ERβ) axis [9, 24, 25] and plant-derived polyphenols, like naringenin [24] and resveratrol [26],upregulate NGB levels, increasing neuron resilience to oxidative stress. Similarly, other hormones and growth factors (e.g. vascular endothelial growth factor, VEGF; brain-derived neurotrophic factor BDNF; erythropoietin, EPO) [27–29], synthetic steroids (e.g. tibolone [30]and other phytochemicals [31]), have been demonstrated to increase NGB levels promoting its cytoprotective function.

Concurrently with investigations on the modulation of NGB, the dissection of its molecular mechanisms of action has revealed a dynamic landscape. Numerous studies have unveiled a complex distribution of NGB across different cellular compartments, and interconnected functions of this globin within and between these compartments [5, 6].

Adding further complexity to this scenario, NGB has been detected in exosomes derived from rat astrocytes, leading to the hypothesis of a potential neuroprotective transfer of the globin among brain cells [32]. Moreover, in the context of breast cancer, we proved the extracellular release of NGB in both cellular and tissue models, providing evidence of its specific modulation by exogenous compounds and suggesting a potential functional role of this globin as a paracrine resilience factor [33]. Therefore, these findings suggest that NGB neuroprotective effects cannot be solely attributed to its cell-autonomous functions; rather they raise the hypothesis that extracellular NGB accumulation could influence neighboring cells. In turn, we addressed here the possibility that dynamic NGB distribution and function extends beyond the physical boundaries of the cell. To this aim, we utilized the neuroblastoma SH-SY5Y cells, which represent a widely employed model for exploring neurodegenerative-related stress and NGB function, to analyze NGB release and effects, in response to physiopathological stimuli.

RESULTS

Evidence of NGB extracellular release in SH-SY5Y cells

Well-known inducers of high levels of intracellular NGB (as 17β-estradiol (E2), resveratrol (Res), and the oxidative stressor hydrogen peroxide (H_2O_2), could redistribute the globin extracellularly in SH-SY5Y treated conditioned medium (CM) and within the fraction of extracellular vesicles (EVs), confirming that the intracellular protein is part of the cell secretome (Supplemental Figure S1). To verify that the induction of high NGB levels culminates with its release in the extracellular milieu, the modulation of NGB release in the extracellular milieu was assessed in the context of ectopic intracellular expression of the protein by using SH-SY5Y cells stably transfected with the plasmid encoding for hemagglutinin (HA) tagged NGB (SH-SY5Y NGB-HA). As depicted in Fig.1A, the high expression of the NGB inside transfected cells is paralleled with a great protein accumulation in the CM. Specifically, the dot blot analysis conducted on CM obtained from both wild type (WT) and NGB-HA SH-SY5Y cells, in conjunction with a recombinant-NGB dose-curve, highlights the release of an average of 102,39 ng ($\pm$ 19,96) of NGB per million overexpressing cells, in contrast to the barely detectable levels of extracellular protein derived from WT cells (Fig. 1B). Furthermore, both the fraction of EVs and that related to EVs-deprived CM obtained from NGB-overexpressing cells show a significant increase in NGB content (Fig. 1C), confirming that, when overexpressed, NGB is released as soluble and vesicle-embedded protein. Isolated EVs were further characterized by morphological analysis using scanning (SEM) and transmission (TEM) electron microscopy (Fig.1D, E). Obtained analysis reveals an EVs population with an average diameter ranging from 31.6 to 113.75 nm in the case of that collected from WT cells, and from 39.81 to 104.76 nm for EVs derived from NGB overexpressing cells (Fig. 1F). Since the exact origin for EV biogenesis (i.e., endosomal or plasma membrane) of collected EVs could not be clearly defined and the lack of consensus-specific markers [34], in this study, accordingly to the size-based classification, we will use the term "small extracellular vesicle (sEVs)", which encompasses the exosomal fraction, to refer to the obtained vesicles.

Altogether, the reported findings confirm that overexpression of the protein inside cells also promotes the redistribution of the protein in extracellular compartments. Hence, the different extracellular fractions (total CM, sEVs, and EVs-deprived CM) obtained from WT and NGB-overexpressing cells were used for assessing the functional protective role of cell-derived extracellular NGB.

Effect of cell-derived extracellular NGB on SH-SY5Y under oxidative stress conditions

To test the hypothesis of a cytoprotective function of cell-derived extracellular NGB, complete CM enriched with extracellular NGB (CM NGB+) was used as pre-treatment (4 h) before administering the oxidative stress by using the CM obtained from WT cells (CM WT) as control. Considering the average release of 102.39 ng of NGB per million SH-SY5Y NGB-HA cells, a concentration of extracellular NGB in CM NGB+ in the nanomolar range (~0,75 nM) was estimated. The effect of long-term stimulation with a toxic dose of H_2O_2 (100 μM, 24 h) in reducing the number of viable cells was prevented only by pre-stimulation with CM NGB+ supporting a protective function of the media (Fig. 2A). This result was also validated by the cytotoxicity assay performed with propidium iodide (PI) staining (Fig. 2B). Notably, neither WT nor NGB+ CM appear to affect cell number under the unstressed condition at the time considered.

To further explore if the reported effects of NGB-enriched CM were due to a direct impact on the apoptotic pathway, the cleavage of the PARP-1 protein into the 89 kDa fragment which represents a common hallmark of apoptotic cell death [35], was also assessed by Western blot. As depicted in Fig.2C, cell culturing with CM WT and CM NGB+ does not impact PARP-1 cleavage under unstressed conditions, whereas pre-stimulation with CM NGB+ before H_2O_2 prevented the generation of the apoptotic 89 kDa fragment induced by the treatment with H_2O_2 (100 μM, 24 h) alone or in combination with prior exposure to CM WT.

The gathered data, combined with the well-recognized role of up-regulated intracellular NGB in promoting mitochondrial functionality, bolstering the resilience to stress, and inhibiting intrinsic apoptosis pathway [7] prompted us to evaluate the impact of CM NGB+ on mitochondrial morphology and dy-

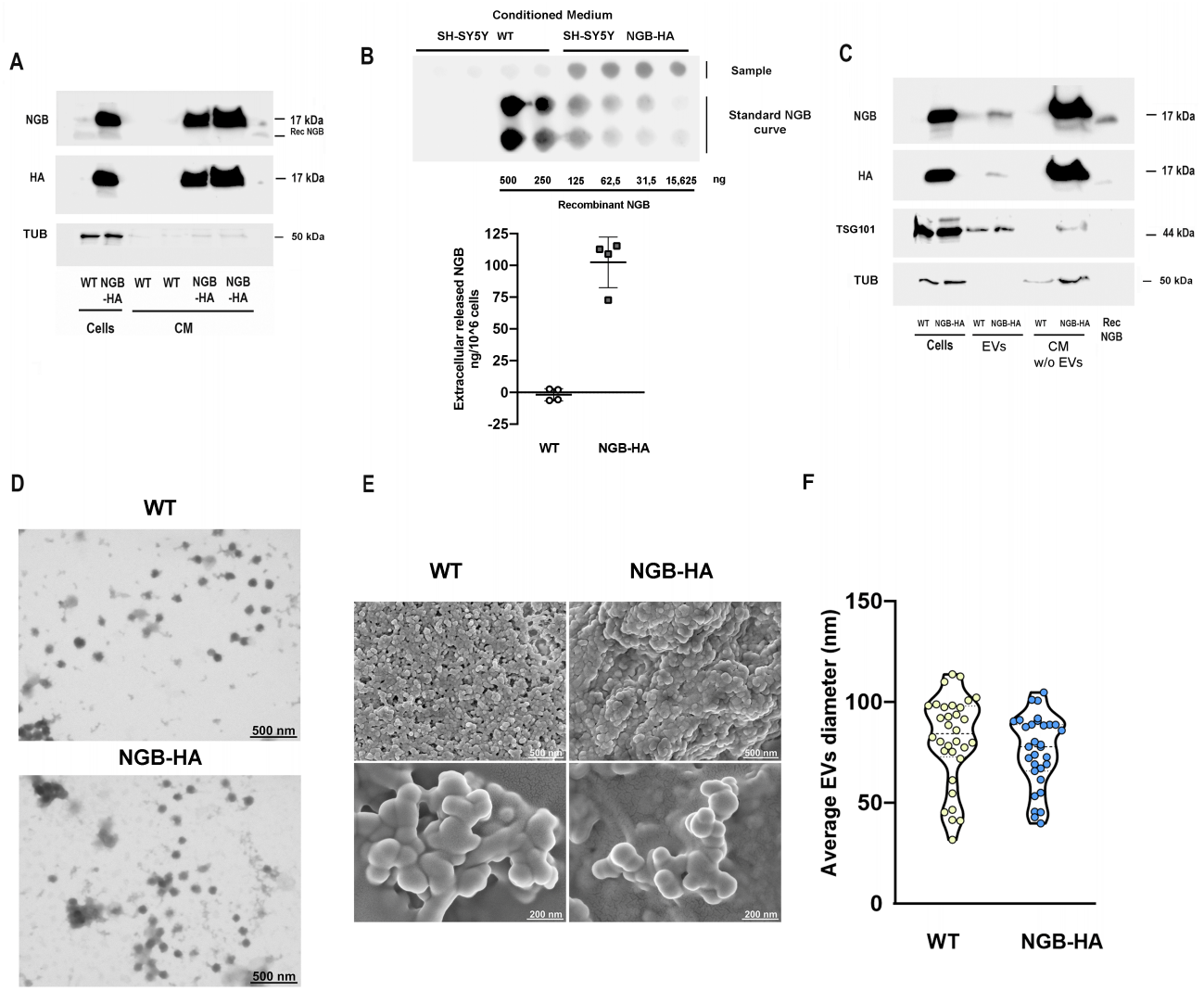

FIGURE 1 ● **Effects of NGB overexpression on extracellular globin release.** NGB and HA levels were measured by Western blot in conditioned medium (**A**) or in EVs and in conditioned medium deprived from EVs (CM w/o EVs) (**C**) obtained from SH-SY5Y wild type (WT) or overexpressing NGB-HA (NGB-HA) cells. Cell lysates were used as control. The levels of tubulin were evaluated on the same filter as cell lysate loading control or as marker of passively released protein in CM. The common exosomes marker TSG101 was used as loading control for EVs (**C**). Where indicated, recombinant NGB protein (2.5 ng) was used as a control. Blot images are representative of at least three independent experiments with similar results. Dot blot analysis (Top) and relative quantification of concentration (Bottom) of extracellular NGB in conditioned media obtained from WT and NGB-HA SH-SY5Y cells in quadruplicate (**B**). NGB recombinant concentration curve was used as dose reference for evaluating the concentration of extracellular NGB. Electron microscopy investigations confirmed the spheroidal morphology of EVs obtained from WT and NGB-HA overexpressing cells as can be observed both in representative STEM micrographs of EVs adsorbed on TEM grids (**D**) as well as in representative SEM micrographs of EVs mounted on silicon wafers (**E**). STEM images were used to analyze the diameter distribution of EVs obtained from WT and NGB-HA overexpressing cells (**F**).

namics under pro-oxidative conditions. In particular, as the mitochondrial alteration occurs early during the apoptotic pathway [36], the morphological analysis of mitochondrial structure was performed by applying confocal microscopy experiments on cells exposed to H_2O_2 stimulation for a short term (4 h). The Mitochondrial Network Analysis tool (MiNA) [37] was used for identifying and quantifying mitochondrial features as the length of mitochondrial branches (branch length mean; summed branch lengths mean) and mean network size (network branches mean), for delineating network elongation and branching status, respectively. Oxidative stress imposed on cell culture determines a significant reduction of all mitochondrial descriptors taken under consideration (**Fig. 2D, 2D′, D″, D‴**), consistently with the fragmented mitochondrial status that occurs during apoptotic pathway activation and mitochondrial dysfunction [38, 39]. Under the reported experimental conditions the CM enriched in NGB enhances both the mean branch length and the summed mean length when compared to H_2O_2 stimulation alone or in the presence of pre-treatment with CM WT (**Fig. 2D′, D″**). On the other hand, neither the treatment with CM NGB+ nor the stimulation with CM WT affect the reduction in the size of the mitochondrial network (**Fig. 2 D‴**),

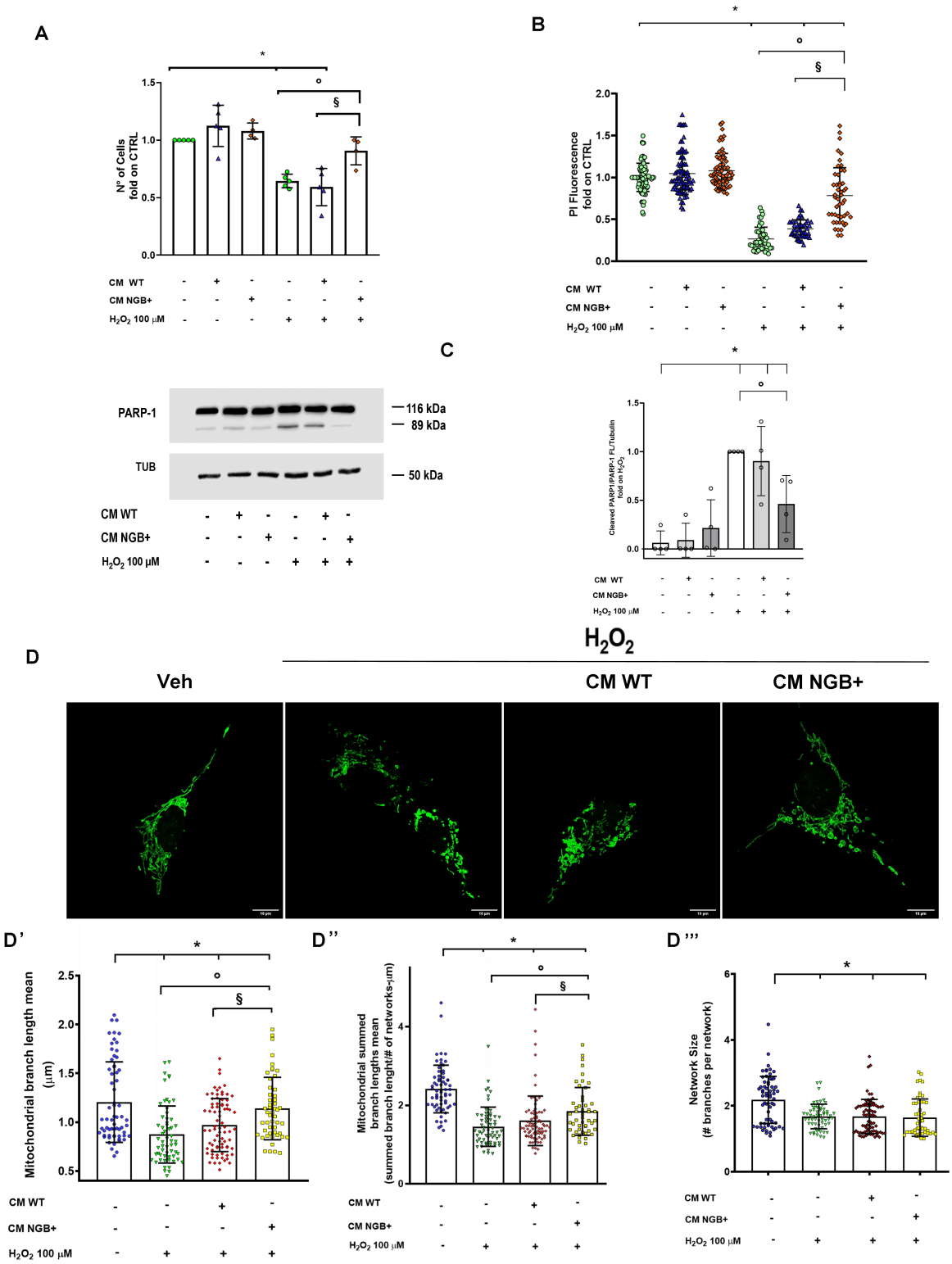

FIGURE 2 ● **Effect of NGB-enriched CM on H_2O_2 induced stress.** The analysis of cytotoxicity on SH-SY5Y cells under the 24 h stimulation with H_2O_2 (100 μM) in presence of pre-treatment (4 h) with CM obtained from WT cells (CM WT) or from NGB-HA overexpressing cells (CM NGB+) was performed by both viable cell counting (**A**) and by the analysis of cell DNA content obtained by propidium iodide assay on fixed and permeabilized cells (**B**). At the same experimental condition, the PARP-1 cleavage was evaluated by Western blot (**C**). The levels of cleaved PARP-1 were normalized to the full-length PARP-1 and tubulin levels on the same filter. Representative blot (left) and densitometric analysis (right) were obtained from at least four independent experiments. Representative image obtained by confocal microscopy showing mitochondrial networks in mEFP-mitochondria SH-SY5Y cells (SH-SY5Y mito-mEFP) treated with Vehicle or with H_2O_2 (100 μM) for 4 h in presence or absence of 4 h pre-treatment with CM from WT SH-SY5Y (CM WT) or NGB-HA overexpressing SH-SY5Y (CM NGB+) (**D**). Mitochondrial morphology features including the branch length mean (**D'**), summed branch lengths mean (**D''**) and mean network size (network branches mean) (**D'''**) were quantified using the Mitochondrial Network Analysis tool (MiNA) on confocal microscopy acquired images. Data shown are means ± SD from ~ 60 cells from 3 independent experiments. In all cases, statistical significance was determined with ANOVA followed by Tukey-Kramer post-test vs CTRL condition (*), vs H_2O_2 condition (°) or vs treatment with H_2O_2 and CM WT (§).

Analysis of the effects of NGB-enriched sEVs and EVs-deprived conditioned medium on SH-SY5Y under oxidative stress

Next, we examined the function of the sEVs and the EVs-deprived CM fraction derived from complete CM NGB+. As depicted in Figure 3A the cell pre-treatment (4 h) with NGB-enriched CM deprived of EVs (CM NGB+ w/o EVs) appears to reduce the apoptotic cleavage of PARP-1 protein occurring after long-term exposure (24 h) to H_2O_2. Although this reduction is not significant with respect to the H_2O_2 treatment, our observation sustains a potential anti-apoptotic role of such fraction. Indeed, when assessing mitochondrial morphology, CM enriched in extracellular NGB mitigates mitochondrial fragmentation (Fig. 3B, B′, B″, B‴), as demonstrated by the significant increase in both the mean and the total summed mean length of branches with respect to the pro-oxidative conditions (Fig. 3B′, B″) while no changes were detected in the network size (Fig. 3B‴). Conversely, pretreatment with CM obtained from WT cells (CM WT w/o EVs) does not induce significant changes in the fragmentation of mitochondrial networks caused by H_2O_2 exposure (Fig. 3B, B′, B″, B‴).

In parallel, because the sEVs subpopulation isolated from NGB+ CM (4 h pre-treatment) rescues the reduction in cell number induced by H_2O_2 stimulation in a dose-dependent manner (Supplemental Figure S2), we tested the potential cytoprotective impact of vesicle-embedded NGB using the most effective dose. For this purpose, we tested the 1.8 μg/mL of sEVs as pre-stimulation before exposure to oxidative stress in the above-described experimental setting. As reported in Fig. 3C, neither sEVs subpopulations obtained from WT cells nor those enriched in NGB (sEVs NGB+) are capable of producing a reduction in PARP-1 cleavage. Nonetheless, the analysis of mitochondrial network status reveals that only NGB-enriched sEVs counteract the mitochondrial fragmentation due to the oxidative stress exposure (Fig. 3D, D′, D″, D‴). In particular, pre-treatment with sEVs NGB+ rescues the decrease of both the length of mitochondrial branches (branch length mean; summed branch lengths mean) (Fig. 3D′, D″) and mean network size (network branches mean) (Fig. 3 D‴) occurring under H_2O_2 treatment. These data suggest that, while complete NGB-enriched secretome, encompassing vesicle-embedded and soluble NGB, shows a greater synergistic effect in promoting overall cell survival against oxidative stress, both fractions of extracellular globin can independently counteract mitochondrial dysfunction under stress conditions and thereby enhance cell resilience.

Analysis of the effects of NGB-enriched conditioned medium on SH-SY5Y under mitochondrial toxicity

Because the obtained results indicate that soluble and vesicle-NGB regulate mitochondrial structure under oxidative stress, we next examined if the extracellular occurrence of NGB can be protective during mitochondrial toxicity. In particular, given the greater protective effect of CM enriched with both soluble and vesicle NGB against oxidative stress (Fig. 2), we tested the effect of the complete secretome from WT and NGB-overexpressing cells in the presence of 3-nitropropionic acid (3-NP), a fungal and plant mitochondrial toxin commonly used to induce the molecular, cellular and phenotypic changes occurring in Huntington's disease (HD) [40]. Specifically, at the cellular level, 3-NP inhibits the complex II (succinate dehydrogenase, SDH) of the respiratory electron transfer chain leading to cell death through the induction of mitochondrial defects [41, 42].

As expected, 24 h administration of 3-NP (15 mM) to SH-SY5Y triggers a significant increase of PARP-1 cleavage confirming the apoptotic pathway activation under chemically induced mitochondrial dysfunction (Fig. 4A). Consistent with previous results, neither WT nor NGB enriched CM modify the level of PARP-1 cleavage in the absence of stress. Conversely, only the pre-treatment with complete CM enriched in NGB shows a significant effect on the reduction of this apoptotic marker (Fig. 4A). Accordingly, the analysis of mitochondrial descriptors reveals that the reduction of the mitochondrial elongation (branch length mean; summed branch lengths mean) and branching (network size) induced by 3-NP was partially attenuated by only the NGB enriched CM (Fig 4B, B′, B″, B‴), indicating a greater effect of CM NGB+ in preventing the mitochondrial fragmentation and the late apoptotic events.

DISCUSSION

Since the year of its discovery in 2000 [4], the physiological functions of the monomeric heme-globin NGB and its cellular/intracellular distribution have been a matter of debate. Continuously emerging evidence adds complexity to the understanding of this fascinating protein. In this panorama, a growing body of evidence supports the definition of NGB as a conserved inducible protein whose accumulation upon physiological and pathological stimuli endows the protein with the capacity to trigger neuroprotective functions under different types of insults (for comprehensive reviews, please refer to [5–7, 43]). *In vitro* and *in vivo* models for physiologically induced or overexpressed NGB have elucidated the role of this globin as a stress-compensating protein. NGB actively participates in fostering homeostatic and pro-survival mechanisms, enabling cells, including neurons and non-neuronal cells, to effectively overcome stressful conditions [15, 18, 44–48].

Besides the connection between the intracellular distribution of NGB and its multifaceted functional roles [6, 7, 15, 25, 48, 49], recent evidences have provided the possibility of the extracellular occurrence of the globin [32, 33, 49].

Here we report that SH-SY5Y cells can release NGB in extracellular culture medium in particular under exposure to inducers of the intracellular globin, as further supported by the presence of the globin within sEVs released by cells in response to treatments with either endogenous inducers (i.e., E2 or hydrogen peroxide) or with exogenous inducer (i.e., resveratrol).

This evidence suggests that NGB accumulation outside cells could represent a potential response to physiological and pathological stimuli enlarging the perspective on NGB properties as an inducible protein and sustaining the idea of a possible role of NGB in the extracellular milieu. Here we took advantage of the evidence of extracellular accumulation of NGB in CM and sEVs derived from NGB-overexpressing cells, to set up a model capable of replicating a quasi-physiological effect of the extracellular NGB accumulation. In particular, we explored the role of extracellular medium enriched in NGB under pro-oxidative conditions and mitochondrial toxicity for modeling stressing cues that commonly correlate with neurodegeneration hallmarks [50]. Reported results demonstrated that the complete CM where NGB accumulates as both soluble

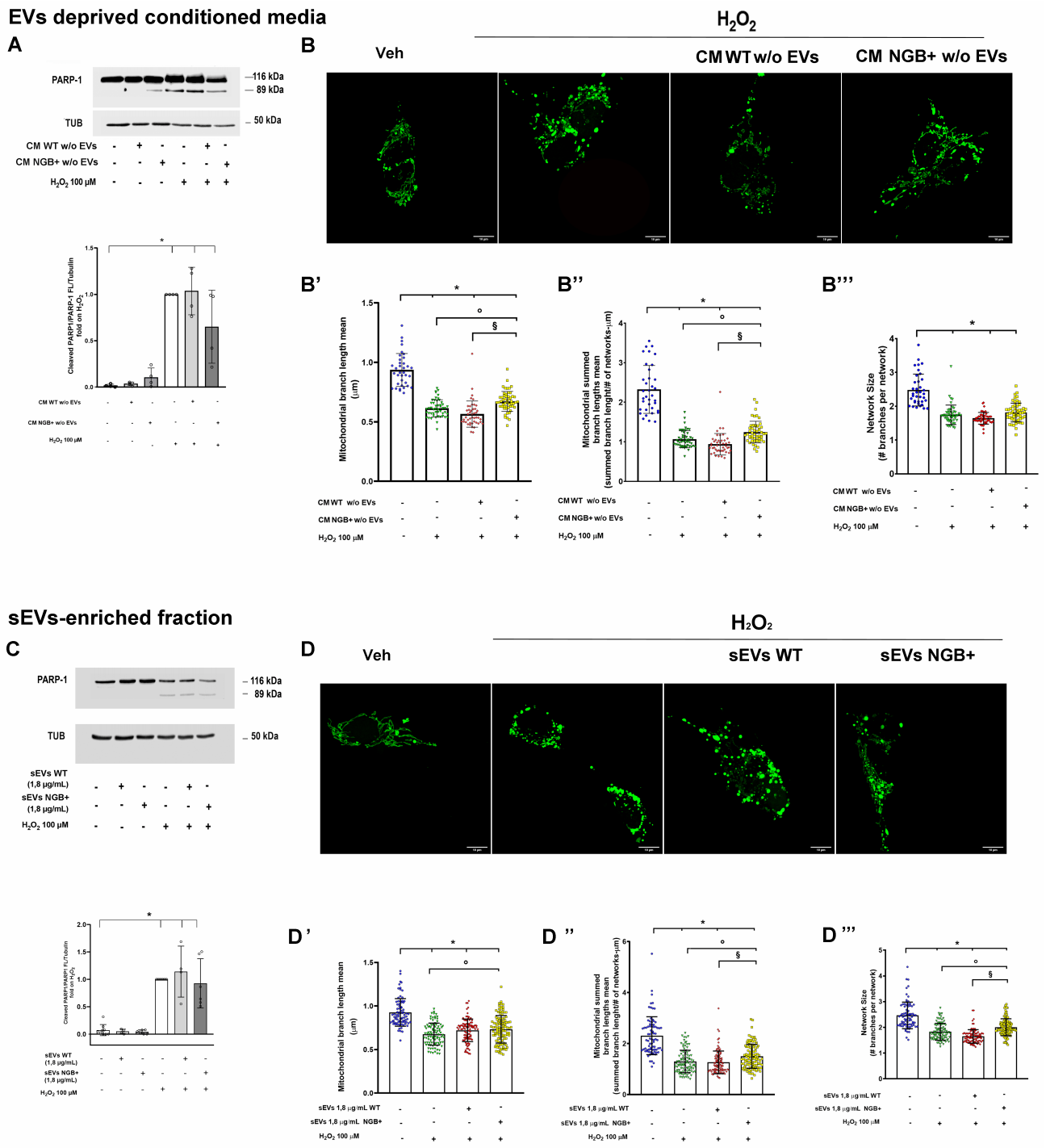

FIGURE 3 ● Effect of EVs- deprived CM and sEVs on H_2O_2 induced cell death and mitochondrial disruption. The level of PARP-1 cleavage was evaluated by Western blot in SH-SY5Y cells pre-treated (4 h) with CM deprived from EVs fraction generated by SH-SY5Y WT (CM WT w/o EVs) or NGB overexpressing cells (CM NGB+ w/o EVs) before the stimulation with H_2O_2 (100 μM; 24 h) (**A**). Representative Western blot (top) and relative densitometric analyses (bottom) are reported. Confocal microscopy representative images of mEFP-mitochondria SH-SY5Y cells (SH-SY5Y mito-mEFP) treated with Vehicle or with H_2O_2 (100 μM) for 4 h in presence or absence of 4 h pre-treatment with CM WT w/o EVs or CM NGB+ w/o EVs (**B**). Mitochondrial branch length mean (**B'**), summed branch lengths mean (**B"**) and mean network size (mitochondrial branches per network) (**B"'**) were quantified using the Mitochondrial Network Analysis tool (MiNA). Western blot analysis of PARP-1 cleavage was performed in SH-SY5Y treated with H_2O_2 (100 μM; 24 h) in presence or absence of pre-treatment with sEVs collected from WT cells (sEVs WT) or NGB-overexpressing cells (sEVs NGB+) at a single dose (1,8 μg/mL) (**C**). Representative Western blot (top) and relative densitometric analyses (bottom) are reported. Representative confocal images of SH-SY5Y with green marked mitochondria (SH-SY5Y mEFP mitochondria) pre-treated with sEVs WT or sEVs NGB+ (1,8 μg/mL; 4 h) before H_2O_2 (100 μM; 4 h) stimulation (**D**). The measure of mitochondrial branch mean length (**D'**), summed branch mean length (**D"**) and mean network size (**D"'**) are reported. For Western blot analysis, the levels of cleaved PARP-1 were normalized to the full-length PARP-1 and tubulin levels on the same filter. Representative blots and densitometric analysis were obtained from at least four independent experiments. For the analysis of mitochondrial morphology, about 60 cells from three independent experiments were analyzed. Data shown are means ± SD. In all cases, statistical significance was determined with ANOVA followed by Tukey-Kramer post-test vs CTRL condition (*), vs H_2O_2 condition (°) or vs treatment with H_2O_2 and CM WT (§).

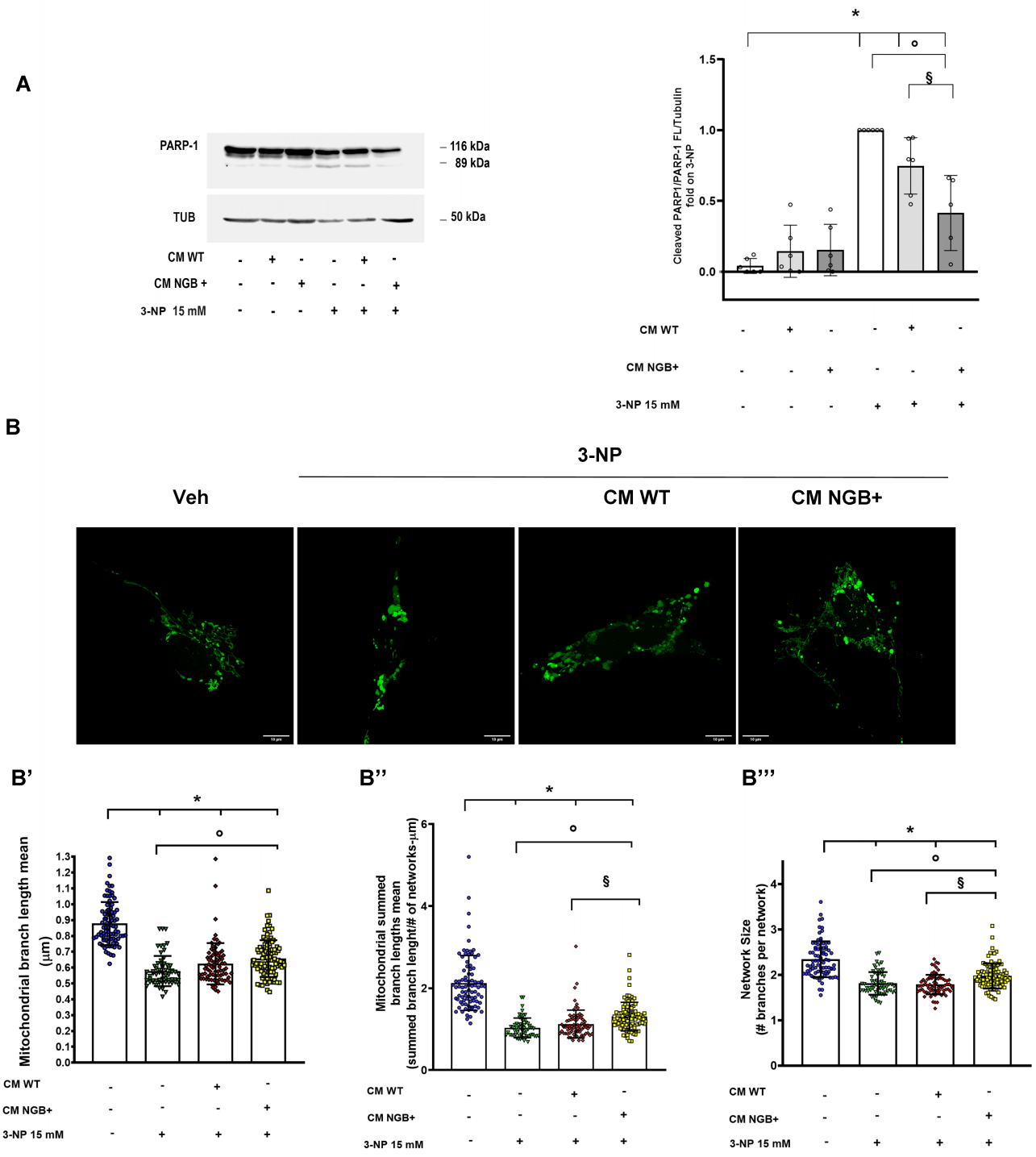

FIGURE 4 ● **Effects of NGB-enriched conditioned media on 3-NP induced mitochondrial toxicity .** Representative Western blot showing the level of cleavage of PARP-1 in SH-SY5Y cells treated with the mitochondrial toxin 3-Nitropropionic acid (3-NP; 15 mM; 24 h) in presence or absence of pre-stimulation (4 h) with CM WT or CM NGB+ (**A**). Fluorescence image of SH-SY5Y mito-mEFP cells pre-stimulated with CM WT of CM NGB+ (4 h) before the exposure to 3-NP toxicity for 4 h (**B**). Bar graphs report the mitochondrial branch length mean (**B'**), summed branch lengths mean (**B''**) and mean network size (**B'''**) obtained by the analysis of about 60 cells from three independent experiments. For Western blot analysis, representative blot (left) and relative densitometric analysis (right) obtained from at least four independent experiments are reported. The levels of cleaved PARP-1 were normalized to the full-length PARP-1 and tubulin levels on the same filter. In all cases, statistical significance was determined with ANOVA followed by Tukey-Kramer post-test vs CTRL condition (*), vs 3-NP condition (°) or vs treatment with 3-NP and CM WT (§).

protein and within EVs, increases cell viability by hampering the activation of the apoptotic cascade in the presence of oxidative stress or induced by specific mitochondrial aberration.

Furthermore, in the context of exploring the cytoprotective effects of extracellular NGB, the examination of mitochondrial network structure in recipient cells exposed to stress conditions has offered further insights. Mitochondrial morphology is characterized by a dynamic equilibrium between the fission and fusion events, leading to fragmented or elongated mitochondrial structures, respectively [51]. Mitochondrial reshaping commonly occurs as a mechanism of cellular response to stress [51, 52], and though stress and cell-specific events may occur [51], it is recognized that mitochondrial fission represents a key part of the apoptotic process induced by severe stress conditions whilst elongated mitochondria can protect against stressors [38, 51, 53, 54]. According to previous findings [42, 55, 56], stimulation with both oxidative stress and the mitochondrial toxin 3-NP leads to mitochondrial fragmentation as a sign of organelle dysfunction and apoptosis activation. In this context, we identified that the cytoprotective effects of NGB-enriched secretome parallel with significant mitigation of the stress-induced damage of the mitochondrial structure, as suggested by the partial recovery of features used for delineating the status of the mitochondrial network. Notably, obtained results suggest that similarly to what has already been proved for the high levels of intracellular NGB [13, 18, 21, 25, 48, 57], also extracellular NGB can intervene in promoting cell survival by preserving the mitochondrial structure and functionality. Indeed, although reported evidence indicates that the NGB-enriched EVs-deprived soluble fraction and sEVs do not significantly rescue cells from late apoptotic events (i.e., PARP-1 cleavage), they fully maintain the capability to counteract mitochondrial fragmentation. These findings suggest, on one hand, that both soluble and vesicle NGB enriched fractions may independently retain a cytoprotective effect under stressing conditions and, on the other hand, that they may synergize to enhance the pro-survival potential of the extracellular globin, warranting in-depth investigations into the cytoprotective contribution of sEVs carrying NGB. In addition, it is worth considering the possibility that sEVs derived from NGB-overexpressing cells may be more effective in carrying their neuroprotective cargo at higher doses, according to the concept of a concentration-dependent biological effect of EVs [58]. In summary, while further research is mandatory to fully validate the neuroprotective potential of extracellular NGB and, particularly, of both the soluble fraction and NGB-enriched sEVs, obtained findings suggest that secretome derived from NGB-overexpressing cells comes to improve SH-SY5Y resilience under stressing conditions.

Previous results obtained in astrocyte cells have led to speculate that the glioprotective effects of extracellular NGB against oxidative stress may occur through the direct regulation of G protein-coupled receptor (GPCR) [59]. Aside, the protective mechanism of extracellular NGB can rely on the delivery of the protein inside the recipient cells where it may accumulate and retain its biological function in keeping homeostasis and activating pro-survival mechanisms. The ability to cross efficiently biological membranes has been previously demonstrated only for zebrafish and human/zebrafish chimeric NGB [60], or for the human protein linked to the HIV transactivator of transcription protein transduction domain (TAT-NGB) [61–63]. Nonetheless, a recent study has shown that intravitreal injection of recombinant NGB, without the use of cell-penetrating peptides (CCP) or chimeric proteins, can restore the endogenous retinal levels of the globin under hypoxic conditions. This treatment also prevents apoptotic cell death and inflammation [64], suggesting that soluble NGB can be effectively internalized and maintain its biological functionality.

Bulk and receptor-mediated endocytosis represents a conserved cellular mechanism operating a critical role in cell communication with the extracellular environment, encompassing the uptake of extracellular nutrients and bioactive macromolecules like proteins [65, 66]. Despite the endosomal internalized cargo degradation to the lysosome is thought to be the predominant fate, some examples of exogenous proteins that are cytosolic delivered and retain their biological activity in recipient cells have been reported [67–69]. Similarly, EVs are lipid bilayer structures acting in inter-cellular trafficking of bioactive molecules whose uptake is considered to prevalently rely on endocytosis [70–72]. Even though non-functional cargo delivery by EVs occurs because of its retainment in the endosomal compartment before the degradation or the re-release, different evidence supports the concept of a functional internalization of the EVs cargo in the cytoplasm of recipient cells [72, 73]. Furthermore, also the direct fusion of EVs with plasma membrane with the consequent cytosolic release of their contents has been reported [70, 72, 74]. Whether similar pathways could apply to extracellular soluble and vesicular NGB certainly warrants further investigation in future studies.

Moreover, several pieces of evidence suggest that the cargo of EVs reflects the condition of the cells from which they originate [70, 71, 74–77], and this concept can generally be extended to the dynamic secretome [78]. Then, it might be possible that NGB overexpression inside cells may provide a parallel modification of cell secretome and sEVs biological cargo. Thus, other neuroprotective factors (e.g. proteins, microRNA) released by NGB overexpressing cells can contribute to the effects of extracellular NGB in fostering the ability of neighboring cells to overcome stressful conditions. While a thorough investigation into such possible indirect non-cell autonomous function of NGB is necessary, our observation of an increase in intracellular NGB levels in cells cultured with NGB-enriched conditioned media that was not interfered by protein translation inhibitor cycloheximide (CHX) (Supplemental Figure S3) supports the notion that the protective role of extracellular NGB could be achieved through its accumulation within recipient cells where the globin can retain its functional properties toward the promotion of mitochondrial and, in turn, cellular resilience.

Overall, the findings reported here offer novel insights into the function of NGB in conveying cellular resilience demonstrating that: i) NGB can be released outside cells both in the soluble and vesicle-embedded form; ii) accumulation of NGB in the extracellular milieu intervene in preserving the mitochondrial structure and preventing the apoptotic cell death induced by oxidative stress or direct mitochondrial toxicity. Such evidence suggests that NGB can amplify its neuroprotective and physiological function beyond the cell boundaries and pave the way for future investigation into the neuroprotective potential of extracellular NGB delivery.

MATERIAL AND METHODS

Reagents

E2, Dulbecco's modified medium (DMEM) with and without phenol red, Fetal Bovine Serum (FBS), G418, hydrogen peroxide H_2O_2, HEPES solution, Hygromycin-B , L-glutamine, MEM Non-essential aminoacids solution, 3-nitropropionic acid (3-NP), NaCl, Resveratrol (Res), Pen-Strep solution, PBS, propidium iodide (PI), protease inhibitor cocktail, Sodium Dodecyl Sulphate SDS, Sodium-Pyruvate, Trypsin-EDTA, Tris buffer, AMICON Ultra-0.5 and AMICON ULTRA-15 centrifugal filter unit with 3.5 KDa cut-off, Fluoroshield™ with DAPI (F6057) anti-NGB (N7162), and anti-Tubulin (T9026) antibodies were obtained from MERCK (Darmstadt, Germany). Bradford protein assay and the chemiluminescence reagent for Western blot superpower ECL were purchased from Bio-Rad (Hercules, CA, USA). The anti-PARP-1 antibody (9542S) was obtained from Cell Signalling Technology Inc. (Beverly, MA, USA) and the anti-TSG101 (GTX70255) antibody was achieved by GeneTex (Irvine, California, USA). Anti-NGB (13499-1-AP) antibody used for dot blot analysis was purchased from Proteintech (Rosemont, Illinois, USA). Recombinant NGB (RD172043100-B) was obtained from BioVendor (Karasek, Czech Republic). Human NGB/Neuroglobin Gene ORF cDNA clone expression plasmid, C-HA tag (Cat# HG15110-CY) was purchased from Sino Biological (Beijing, China). mEmerald-Mito-7 was a gift from Michael Davidson (Addgene plasmid # 54160; http://n2t.net/addgene:54160; RRID:Addgene_54160) [79]. Analytical or reagent grade products were used without further purification.

Cell Culture

Human neuroblastoma cells SH-SY5Y (American Type Culture Collection, LGC Standards S.r.l., Milan, Italy) were grown in air containing 5% CO_2, using DMEM, with or without phenol red, containing 10% (v/v) fetal bovine serum, L-glutamine (2 mM), Sodium-Pyruvate (1%), HEPES solution (1%), non-essential aminoacids (1%) and Pen-Strep solution (Penicillin 100 U/mL and Streptomycin 100 mg/mL). Cells were passaged twice a week and were used in passages 4-8. Cell line authentication was performed periodically by amplification of multiple STR loci by BMR (Padua, Italy). Cells were treated for the indicated time with either vehicle (EtOH/PBS 1:2), H_2O_2 (50 and 100 μM), 3-NP (15 mM), E2 (1 nM), Res (100 nM), conditioned media or sEVs in free phenol-red DMEM. For what concerning the experiments involving the stimulation with conditioned media or sEVs, cells were pretreated for 4 h before the stimulation with H_2O_2 or 3NP. Unless otherwise indicated, cells were seeded at a density of $2.5x10^5$ in 6-well plates and treated as described.

Generation of NGB-overexpressing and mEmerald-Mito-7 SH-SY5Y models

For the generation of SH-SY5Y cell stable overexpressing NGB with HA tag cells were grown to ~70% confluence and then were transfected with pCMV3-NGB-HA (Sino Biological, Beijing, China), using lipofectamine reagent (Invitrogen, Carlsbad, CA, USA), according to the manufacturer's instructions. After the selection with Hygromycin-B (600 μg/mL) cells were tested for the expression of NGB-HA. The same protocol was applied for generating SH-SY5Y with stable fluorescent labeled mitochondria generation: in particular, cells were transfected with mEmerald-Mito-7 plasmid (Addgene plasmid #54160; a gift from Michael Davidson) and selected with G418 (400 μg/mL). The mitochondrial labeling was tested by immunofluorescence microscopy.

Generation of conditioned media

For the generation of conditioned media, NGB-overexpressing SH-SY5Y and WT SH-SY5Y were seeded ($2,5 \times 10^6$) in 100 mm culture dish and then were serum starved (0%) in phenol red-free medium overnight. Cells were then washed twice with PBS and were cultured in fresh serum-starved and phenol red-free medium (10 mL) for 24 h. After cell culturing, media were collected and centrifuged at 2000 g for 15 min to remove dead cells. Supernatants were filtered using 10 μM cut-off membrane to clean them from cell debris and then frozen at -80 °C until use for cell culturing or concentrated to a final volume of 100 μL by using AMICON ULTRA-15 centrifugal filter unit with 3.5 kDa cut-off membrane, for Western blot analysis of secreted protein. For cell culturing, conditioned media were diluted in 1:1 ratio with fresh medium and added with 10% heat inactivated FBS.

sEVs and conditioned media w/o EVs collection

For analysis of NGB content in extracellular vesicle fraction, SH-SY5Y conditioned media was ultracentrifuged in a Beckman Coulter ultracentrifuge using a SW-32Ti swinging bucket rotor for 20 min at 15.000 g. The supernatant was collected and re-spun at 110.000 g for 150 min. At the end, the supernatant was collected (CM w/o EVs), and the pellet (the sEVs fraction) was incubated on ice for 15 min. The sEVs fraction was re-suspendend in PBS and re-spun at 110.000 g for 150 min. The supernatant was removed, and after 15 min incubation on ice, the pellet was lysed in 50 μl of YY lysis buffer or re-suspendend in PBS for cell stimulation. For cell stimulation, 1:10 of sEVs PBS suspension was lysed in YY lysis buffer and quantified for protein concentration using the Bradford Protein Assay. For cell culturing, CM w/o EVs was diluted in 1:1 ratio with fresh medium and added with 10% heat inactivated FBS.

Confocal microscopy analysis

mEmerald-Mito-7 SH-SY5Y cells seeded on coverslip were rinsed with PBS followed by fixation in formaldehyde 4% for 10 min. Coverslips were mounted on microscope glass slide using Prolong®Gold anti-fade reagent (Invitrogen). Confocal analysis (Z-stack series) was performed using Leica TCS SP5 microscopy (63x Objective, 3X zoom) (Leica Microsystems, Wetzlar, Germany). Maximum intensity projection of each Z-stack series was generated by using the FIJI distribution of ImageJ software for Microsoft Windows (NIH, Bethesda, MD, USA).

For each experiment, Z-stack fluorescence images were loaded into FIJI distribution of ImageJ software in their native format and maximum intensity projection was generated. Images were prepared for the analysis by applying the following pre-processing steps: application of median filtering (1-pixel radius) and "unsharp mask". Images were then processed with Ridge detection. Mitochondrial morphology was analyzed using the Mitochondrial Network Analysis tool (MiNA) [37, 80], a macro tool developed for FIJI distribution of ImageJ software for Microsoft Windows (NIH, Bethesda, MD, USA). Following information were extracted from the morphological skeleton: mean length of network branches (branch length

mean; summed branch lengths mean) and mean network size (network branches mean). Around 60 cells per condition were randomly selected from 3 independent experiments.

For experiment concerning the expression of NGB, following fixation and blocking step with 3% BSA in PBS containing 0.5% of Triton-X100, SH-SY5Y cells were incubated with anti-NGB (final dilution 1:300) o/n at 4°C. After washing with PBS, cells were incubated with Alexa Fluor 546 donkey anti-rabbit secondary antibodies (Carlsbad, CA, USA) (1:300) for 1 h at RT. Coverslips were mounted on microscope glass slide using Fluoroshield with DAPI (Invitrogen). For quantification of NGB protein expression, exposure time was set at the CTRL sample. All images were analyzed by using the FIJI distribution of ImageJ software for Microsoft Windows (NIH, Bethesda, MD, USA) selecting single cells for each acquired field. For each cell, the area and integrated density were measured and then the corrected total cell fluorescence (CTCF) = Integrated Density – (Area of selected cell X Mean fluorescence of background readings) was calculated. Confocal analysis was performed using Nikon A1R (40x objective, 3x zoom) (Nikon Corporation, Tokyo, Japan).

Electron Microscopy

For transmission electron microscopy (TEM) analysis, the sEVS pellets, obtained by differential centrifugation, were fixed for 45 min at 4°C in a mixture of 2% paraformaldehyde and 1.25% glutaraldehyde. Samples were rinsed in PBS and subjected to further centrifugation. The resulting pellets were resuspended in 50 μL of the same buffer, and 5 μL drops were gently deposited on formvar-coated TEM grids, using uranyl acetate as contrasting agent. Grids with adsorbed microvesicles were observed under a Helios Nanolab 600 dual beam (FIB/SEM) microscope, using the STEM detector. For SEM analysis, the same suspension employed to prepare TEM grids was dehydrated with ethanol solutions at increasing concentrations and deposited on a silicon substrate. Silicon wafers hosting EVs were air dried under a fume hood, sputter coated with gold and examined under a Gemini 300 field emission SEM. The average diameter of extracted EVs population were manually performed by using the FIJI distribution of ImageJ software for Microsoft Windows (NIH, Bethesda, MD, USA), on 4 different fields from STEM images from two experiments for each tested condition.

Cell quantification

Propidium iodide (PI) cytotoxicity assay

SH-SY5Y cells were grown up to 80% confluence in a 96-well plate and treated with the selected compounds. To quantify adherent cells for cytotoxicity assessment after stimulation, cells were fixed and permeabilized with cold Ethanol (EtOH) 70% for 15 min at −20°C. EtOH solution was removed, and the cells were incubated with propidium iodide buffer for 30 min in the dark. The solution was removed, and the cells were rinsed with PBS solution. The fluorescence was revealed (excitation wavelength: 537 nm; emission wavelength: 621 nm) with Tecan Spark 20M multimode microplate reader (Tecan, Männedorf, Switzerland).

Cell count

After the treatments, SH-SY5Y cells were detached with 0.5 mL of trypsin-EDTA and collected in 0.5 mL of DMEM with 10% FBS, for a final volume of 1 mL. After centrifugation (300 g, 5 min), cells were re-suspended in DMEM without red phenol (0.5 mL), added with Trypan Blue (0.4%), and then counted with a hemocytometer. The number of viable cells/mL was calculated by taking the average of the number of only viable cells counted in the 3 diagonal quadrants, multiplied by the dilution factor (10^4).

Protein extraction and Western blot assay

Cells or sEVs were lysed with a YY buffer mix (50 mM HEPES pH: 7.5, 10% glycerol, 150 mM NaCl, 1% Triton X-100, 1 mM EDTA, 1 mM EGTA), containing 0.70% (w/v) Sodium Dodecyl Sulphate SDS. Total proteins were quantified using the Bradford Protein Assay. Solubilized protein from sEVs lysate (10-20 μg) and correspondent amount of cell lysate and/or conditioned medium were resolved by 13.5% SDS-PAGE at 100 V for 1 h at 25°C and then transferred on a nitrocellulose using the Trans-Turbo Blot Transfer System (Bio-Rad) for 10 min at 25 V. In Western blot not concerning sEVs, solubilized proteins from cell lysate (30-40 μg), and, when reported, correspondent amount of conditioned media, were resolved by 7% or 13.5% SDS-PAGE and transferred on a nitrocellulose as above reported. The membranes were then blocked with 5% (w/v) filtered BSA or fat-free milk in 138 mM NaCl, 25 mM Tris, pH 7.6, and 0.1 (w/v) Tween 20 at 25°C for 1 h, and then incubated overnight at 4°C with anti-NGB (final dilution 1:1000), anti-PARP-1 (final dilution 1:1000), anti-TSG101 (final dilution 1:1000), and anti-tubulin (final dilution 1:40000). Antibody reactivity was observed with ECL chemiluminescence Western blotting detection reagent, by using a ChemiDoc XRS+Imaging System (Bio-Rad Laboratories, Hercules, CA, USA). The densitometric analysis was performed by ImageJ software for Microsoft Windows (NIH, Bethesda, MD, USA).

Dot Blot assay

SH-SY5Y were seeded (5 X10^5/well) in 6-well plates, then were serum starved in phenol red-free medium overnight. Cells were then washed twice with PBS and were cultured in fresh serum-starved and phenol red-free medium for 24 h. Conditioned media (600 μL), obtained from both WT and NGB-HA SH-SY5Y cells, were spotted into nitrocellulose membrane with Bio-Dot Microfiltration Apparatus (Bio-Rad, Hercules, CA, USA). In addition, recombinant NGB with a note concentration (500 ng/mL) was diluted as 1:2, 1:4, 1:8, 1:16 and 1:32 (final concentrations: 250 – 125 - 62.5 - 31.25 - 15.625 ng/mL, respectively) and spotted into the nitrocellulose membrane in the same manner, to be used as extrapolation marker. The membranes were then incubated overnight at 4°C with anti-NGB (13499-1-AP Proteintech final dilution 1:1000) and the antibody reactivity was observed with ECL chemiluminescence Western blotting detection reagent, by using a ChemiDoc XRS + Imaging System (Bio-Rad Laboratories, Hercules, CA, USA). The densitometric analysis was performed by ImageJ software for Microsoft Windows (NIH, Bethesda, MD, USA). The anti-NGB (13499-1-AP Proteintech) specific staining in detecting NGB overexpressed protein in cell lysate and conditioned medium was tested by Western blot (Supplemental Figure S4).

Statistical Analysis

The statistical analysis was performed by ANOVA followed by Tukey–Kramer post-test with the PRISM 6.01 software system (GraphPad Software, Inc, San Diego, CA, USA) for Windows. In all cases, only values of $p < 0.05$ were considered significant.

ACKNOWLEDGMENTS

We sincerely thank Prof. Jeffrey A Stuart (Brock University, St. Catharines, ON, Canada) for generously sharing his time, guidance, support, and training, which have provided us with the knowledge, expertise, and skills necessary to study mitochondrial morphology and structure using the MiNA tool. We are also grateful to Prof. Filippo Acconcia (Department of Science, University Roma Tre) for his valuable support in data interpretation and discussion.

This research was funded by Grants PRIN 2022 n20223RXEEC CUP: F53D23005240006 to M.M. (Maria Marino). The study reported in figure 1 was supported by "Rome Technopole" - ECS00000024 PNRR Mission 4 -Component 2 CUP:F83B22000040006 to M.M..

SUPPLEMENTAL MATERIAL

All supplemental data for this article are available online at www.cell-stress.com.

CONFLICT OF INTEREST

The authors declare no conflict of interest.

COPYRIGHT

Please cite this article as: Giovanna Bastari, Virginia Solar Fernandez, Maurizio Muzzi, Sandra Moreno, Maria Marino, Marco Fiocchetti (2024). **Neuroglobin-enriched secretome provides neuroprotection against hydrogen peroxide and mitochondrial toxin-induced cellular stress** . **Cell Stress** 8: 99-111. doi: 10.15698/cst2024.11.300

REFERENCES

1. Hotamisligil GS, Davis RJ (**2016**). Cell Signaling and Stress Responses. **Cold Spring Harb Perspect Biol** 8 (10): 6072. doi:10.1101/cshperspect.a006072

2. Kole AJ, Annis RP, Deshmukh M (**2013**). Mature neurons: equipped for survival. **Cell Death Dis** 4 (6): 689. doi:10.1038/cddis.2013.220

3. Farley MM, Watkins TA (**2018**). Intrinsic Neuronal Stress Response Pathways in Injury and Disease. **Annu Rev Pathol Mech Dis** 13 (1): 93–116. doi:10.1146/annurev-pathol-012414-040354

4. Burmester T, Weich B, Reinhardt S, Hankeln T (**2000**). A vertebrate globin expressed in the brain. **Nature** 407 (6803): 520–523. doi:10.1038/35035093

5. Ascenzi P, Masi AD, Leboffe L, Fiocchetti M, Nuzzo MT, Brunori M, Marino M (**2016**). Neuroglobin: From structure to function in health and disease. **Mol Aspects Med** 52: 1–48. doi:10.1016/j.mam.2016.10.004

6. Luyckx E, Van Acker ZP, Ponsaerts P, Dewilde S (**2019**). Neuroglobin Expression Models as a Tool to Study Its Function. **Oxid Med Cell Longev** p 5728129. doi:10.1155/2019/5728129

7. Fiocchetti M, Cracco P, Montalesi E, Fernandez VS, Stuart JA, Marino M (**2021**). Neuroglobin and mitochondria: The impact on neurodegenerative diseases. **Arch Biochem Biophys** 701: 108,823. doi:10.1016/j.abb.2021.108823

8. Dellavalle B, Hempel C, Kurtzhals JAL, Penkowa M (**2010**). In vivo expression of neuroglobin in reactive astrocytes during neuropathology in murine models of traumatic brain injury, cerebral malaria, and autoimmune encephalitis. **Glia** 58 (10): 1220–1227. doi:10.1002/glia.21002

9. De Marinis E, Acaz-Fonseca E, Arevalo MA, Ascenzi P, Fiocchetti M, Marino M, Garcia-Segura LM (**2013**). 17β-Oestradiol anti-inflammatory effects in primary astrocytes require oestrogen receptor β-mediated neuroglobin up-regulation. **J Neuroendocrinol** 25 (3): 260–270. doi:10.1111/jne.12007

10. Lechauve C, Augustin S, Roussel D, Sahel JA, Corral-Debrinski M (**2013**). Neuroglobin involvement in visual pathways through the optic nerve. **Biochim Biophys Acta** 1834 (9): 1772–1778. doi:10.1016/j.bbapap.2013.04.014

11. Li WD, Sun Q, Zhang XS, Wang CX, Li S, Li W, Hang CH (**2014**). Expression and cell distribution of neuroglobin in the brain tissue after experimental subarachnoid hemorrhage in rats: a pilot study. **Cell Mol Neurobiol** 34 (2): 247–255. doi:10.1007/s10571-013-0008-7

12. Dias-Pedroso D, Ramalho JS, Sardão VA, Jones JG, Romão CC, Oliveira PJ, Vieira HLA (**2022**). Carbon Monoxide-Neuroglobin Axis Targeting Metabolism Against Inflammation in BV-2 Microglial Cells. **Mol Neurobiol** 59 (2): 916–931. doi:10.1007/s12035-021-02630-4

13. Antao ST, Duong TTH, Aran R, Witting PK (**2010**). Neuroglobin Overexpression in Cultured Human Neuronal Cells Protects Against Hydrogen Peroxide Insult via Activating Phosphoinositide-3 Kinase and Opening the Mitochondrial KATP Channel. **Antioxid Redox Signal** 13 (6): 769–781. doi:10.1089/ars.2009.2977

14. Li RC, Guo SZ, Lee SK (**2010**). Neuroglobin Protects Neurons against Oxidative Stress in Global Ischemia. **J Cereb Blood Flow Metab** 30 (11): 1874–1882. doi:10.1089/ars.2009.2977

15. Watanabe S, Takahashi N, Uchida H, Wakasugi K (**2012**). Human Neuroglobin Functions as an Oxidative Stress-responsive Sensor for Neuroprotection ⁎. **J Biol Chem** 287 (36): 30,128. doi:10.1074/jbc.M112.373381

16. de Vidania S, Palomares-Perez I, Frank-García A, Saito T, Saido TC, Draffin J, Szaruga M, Chávez-Gutierrez L, Calero M, Medina M, Guix FX, Dotti CG (**2020**). Prodromal Alzheimer's Disease: Constitutive Upregulation of Neuroglobin Prevents the Initiation of Alzheimer's Pathology. **Front Neurosci** 14: 562,581. doi:10.3389/fnins.2020.562581

17. Sun Y, Jin K, Peel A, Mao XO, Xie L, Greenberg DA (**2003**). Neuroglobin protects the brain from experimental stroke in vivo. **Proc Natl Acad Sci** 100 (6): 3497–3500. doi:10.1073/pnas.0637726100

18. Liu J, Yu Z, Guo S, Lee SR, Xing C, Zhang C, Gao Y, Nicholls DG, Lo EH, Wang X (**2009**). Effects of neuroglobin overexpression on mitochondrial function and oxidative stress following hypoxia/reoxygenation in cultured neurons. **J Neurosci Res** 87 (1): 164–170. doi:10.1002/jnr.21826

19. Shao G, Gong KR, Li J, Xu XJ, Gao CY, Zeng XZ, Lu GW, Huo X (**2009**). Antihypoxic effects of neuroglobin in hypoxia-preconditioned mice and SH-SY5Y cells. **Neurosignals** 17 (3): 196–202. doi:10.1159/000209867

20. Gorgun MF, Zhuo M, Dineley KT, Englander EW (**2019**). Elevated Neuroglobin Lessens Neuroinflammation and Alleviates Neurobehavioral Deficits Induced by Acute Inhalation of Combustion Smoke in the Mouse. **Neurochem Res** 44 (9): 2170–2181. doi:10.1007/s11064-019-02856-8

21. Khan AA, Mao XO, Banwait S, Jin K, Greenberg DA (**2007**). Neuroglobin attenuates β-amyloid neurotoxicity in vitro and transgenic Alzheimer phenotype in vivo. **Proc Natl Acad Sci** 104 (48): 19,114–19,119. doi:10.1073/pnas.0706167104

22. Kleinknecht A, Popova B, Lázaro DF, Pinho R, Valerius O, Outeiro TF, Braus GH (**2016**). C-Terminal Tyrosine Residue Modifications Modulate the Protective Phosphorylation of Serine 129 of α-Synuclein in a Yeast Model of Parkinson's Disease. **PLOS Genet** 12 (6): e1006,098. doi:10.1371/journal.pgen.1006098

23. Li Y, Dai Y, Sun J, Xiang Y, Yang J, Dai S, Zhang X (**2016**). Neuroglobin Attenuates Beta Amyloid-Induced Apoptosis Through Inhibiting Caspases Activity by Activating PI3K/Akt Signaling Pathway. **J Mol Neurosci** 58 (1): 28–38. doi:10.1007/s12031-015-0645-z

24. De Marinis E, Ascenzi P, Pellegrini M, Galluzzo P, Bulzomi P, Arevalo MA, Garcia-Segura LM, Marino M (**2010**). 17β-estradiol–a new modulator of neuroglobin levels in neurons: role in neuroprotection against H_2O_2-induced toxicity. **Neurosignals** 18 (4): 223–235. doi:10.1159/000323906

25. De Marinis E, Fiocchetti M, Acconcia F, Ascenzi P, Marino M (**2013**). Neuroglobin upregulation induced by 17β-estradiol sequesters cytocrome c in the mitochondria preventing H2O2-induced apoptosis of neuroblastoma cells. **Cell Death Dis** 4 (2): 508. doi:10.1038/cddis.2013.30

26. Cracco P, Montalesi E, Parente M, Cipolletti M, Iucci G, Battocchio C, Venditti I, Fiocchetti M, Marino M (**2023**). A Novel Resveratrol-Induced Pathway Increases Neuron-Derived Cell Resilience against Oxidative Stress. **Int J Mol Sci** 24 (6): 5903. doi:10.3390/ijms24065903

27. Gao Y, Mengana Y, Cruz YR, Muñoz A, Testé IS, García JD, Wu Y, Rodríguez JCG, Zhang C (**2011**). Different Expression Patterns of Ngb and EPOR in the Cerebral Cortex and Hippocampus Revealed Distinctive Therapeutic Effects of Intranasal Delivery of Neuro-EPO for Ischemic Insults to the Gerbil Brain. **J Histochem Cytochem** 59 (2): 214–227. doi:10.1369/0022155410390323

28. Jin K, Mao X, Xie L, Greenberg DA (**2012**). Interactions between vascular endothelial growth factor and neuroglobin. **Neurosci Lett** 519 (1): 47–50. doi:10.1016/j.neulet.2012.05.018

29. Nuzzo MT, Fiocchetti M, Totta P, Melone M, Cardinale A, Fusco FR, Gustincich S, Persichetti F, Ascenzi P, Marino M (**2017**). Huntingtin polyQ Mutation Impairs the 17β-Estradiol/Neuroglobin Pathway Devoted to Neuron Survival. **Mol Neurobiol** 54 (8): 6634–6646. doi:10.1007/s12035-016-0337-x

30. Barreto GE, Mcgovern AJ, Garcia-Segura LM (**2021**). Role of Neuroglobin in the Neuroprotective Actions of Estradiol and Estrogenic Compounds. **Cells** 10 (8): 1907. doi:10.3390/cells10081907

31. Liu N, Yu Z, Gao X, Song YS, Yuan J, Xun Y, Wang T, Yan F, Yuan S, Zhang J, Xiang S, Lo EH, Wang X (**2016**). Establishment of Cell-Based Neuroglobin Promoter Reporter Assay for Neuroprotective Compounds Screening. **CNS Neurol Disord - Drug Targets- CNS Neurol Disord** 15 (5): 629–639. doi:10.2174/1871527315666160321105612

32. Venturini A, Passalacqua M, Pelassa S, Pastorino F, Tedesco M, Cortese K, Gagliani MC, Leo G, Maura G, Guidolin D, Agnati LF, Marcoli M, Cervetto C (**2019**). Exosomes From Astrocyte Processes: Signaling to Neurons. **Front Pharmacol** 10: 1452. doi:10.3389/fphar.2019.01452

33. Fiocchetti M, Fernandez VS, Segatto M, Leone S, Cercola P, Massari A, Cavaliere F, Marino M (**2020**). Extracellular Neuroglobin as a Stress-Induced Factor Activating Pre-Adaptation Mechanisms against Oxidative Stress and Chemotherapy-Induced Cell Death in Breast Cancer. **Cancers** 12 (9): 2451. doi:10.3390/cancers12092451

34. Théry C, et al (**2018**). Minimal information for studies of extracellular vesicles 2018 (MISEV2018): a position statement of the International Society for Extracellular Vesicles and update of the MISEV2014 guidelines. **J Extracell Vesicles** 7 (1): 1535,750. doi:10.1080/20013078.2018.1535750

35. Gobeil S, Boucher CC, Nadeau D, Poirier GG (**2001**). Characterization of the necrotic cleavage of poly(ADP-ribose) polymerase (PARP-1): implication of lysosomal proteases. **Cell Death Differ** 8 (6): 588–594. doi:10.1038/sj.cdd.4400851

36. Jeong SY, Seol DW (**2008**). The role of mitochondria in apoptosis. **BMB Rep** 41 (1): 11–22. doi:10.5483/bmbrep.2008.41.1.011

37. Valente AJ, Maddalena LA, Robb EL, Moradi F, Stuart JA (**2017**). A simple ImageJ macro tool for analyzing mitochondrial network morphology in mammalian cell culture. **Acta Histochem** 119 (3): 315–326. doi:10.1016/j.acthis.2017.03.001

38. Cho DH, Nakamura T, Lipton SA (**2010**). Mitochondrial dynamics in cell death and neurodegeneration. **Cell Mol Life Sci** 67 (20): 3435–3447. doi:10.1007/s00018-010-0435-2

39. Seager R, Lee L, Henley JM, Wilkinson KA (**2020**). Mechanisms and roles of mitochondrial localisation and dynamics in neuronal function. **Neuronal Signal** 4 (2): 20200,008. doi:10.1042/NS20200008

40. Túnez I, Tasset I, Cruz VPDL, Santamaría A (**2010**). 3-Nitropropionic Acid as a Tool to Study the Mechanisms Involved in Huntington's Disease: Past, Present and Future. **Molecules** 15 (2): 878–916. doi:10.3390/molecules15020878

41. Nishimura M, Okimura Y, Fujita H, Yano H, Lee J, Suzaki E, Inoue M, Utsumi K, Sasaki J (**2008**). Mechanism of 3-nitropropionic acid-induced membrane permeability transition of isolated mitochondria and its suppression by L-carnitine. **Cell Biochem Funct** 26 (8): 881–891. doi:10.1002/cbf.1521

42. Liot G, Bossy B, Lubitz S, Kushnareva Y, Sejbuk N, Bossy-Wetzel E (**2009**). Complex II inhibition by 3-NP causes mitochondrial fragmentation and neuronal cell death via an NMDA- and ROS-dependent pathway. **Cell Death Differ** 16 (6): 899–909. doi:10.1038/cdd.2009.22

43. Exertier C, Montemiglio LC, Freda I, Gugole E, Parisi G, Savino C, Vallone B (**2022**). Neuroglobin, clues to function and mechanism. **Mol Aspects Med** 84: 101,055. doi:10.1016/j.mam.2021.101055

44. Wakasugi K, Nakano T, Morishima I (**2003**). Oxidized Human Neuroglobin Acts as a Heterotrimeric Gα Protein Guanine Nucleotide Dissociation Inhibitor ⁎. **J Biol Chem** 278 (38): 36,505–36,512. doi:10.1074/jbc.M305519200

45. Raychaudhuri S, Skommer J, Henty K, Birch N, Brittain T (**2010**). Neuroglobin protects nerve cells from apoptosis by inhibiting the intrinsic pathway of cell death. **Apoptosis** 15 (4): 401–411. doi:10.1007/s10495-009-0436-5

46. Yu Z, Xu J, Liu N, Wang Y, Li X, Pallast S, Van Leyen K, X W (**2012**). Mitochondrial distribution of neuroglobin and its response to oxygen-glucose deprivation in primary-cultured mouse cortical neurons. **Neuroscience** 218: 235–242. doi:10.1016/j.neuroscience.2012.05.054

47. Yu Z, Zhang Y, Liu N, Yuan J, Lin L, Zhuge Q, Xiao J, Wang X (**2016**). Roles of Neuroglobin Binding to Mitochondrial Complex III Subunit Cytochrome c1 in Oxygen-Glucose Deprivation-Induced Neurotoxicity in Primary Neurons. **Mol Neurobiol** 53 (5): 3249–3257. doi:10.1007/s12035-015-9273-4

48. Manganelli V, Salvatori I, Costanzo M, Capozzi A, Caissutti D, Caterino M, Valle C, Ferri A, Sorice M, Ruoppolo M, Garofalo T, Misasi R (**2021**). Overexpression of Neuroglobin Promotes Energy Metabolism and Autophagy Induction in Human Neuroblastoma SH-SY5Y Cells. **Cells** 10 (12): 3394. doi:10.3390/cells10123394

49. Fernandez VS, Fiocchetti M, Cipolletti M, Segatto M, Cercola P, Massari A, Ghinassi S, Cavaliere F, Marino M (**2021**). Neuroglobin: A New Possible Marker of Estrogen-Responsive Breast Cancer. **Cells** 10 (8): 1986. doi:10.3390/cells10081986

50. Wilson DM, Cookson MR, Van Den Bosch L, Zetterberg H, Holtzman DM, Dewachter I (**2023**). Hallmarks of neurodegenerative diseases. **Cell** 186 (4): 693–714. doi:10.1016/j.cell.2022.12.032

51. Eisner V, Picard M, Hajnóczky G (**2018**). Mitochondrial dynamics in adaptive and maladaptive cellular stress responses. **Nat Cell Biol** 20 (7): 755–765. doi:10.1038/s41556-018-0133-0

52. Zemirli N, Morel E, Molino D (**2018**). Mitochondrial Dynamics in Basal and Stressful Conditions. **Int J Mol Sci** 19 (2): 564. doi:10.3390/ijms19020564

53. Otera H, Ishihara N, Mihara K (**2013**). New insights into the function and regulation of mitochondrial fission. **Biochim Biophys Acta BBA - Mol Cell Res** 1833 (5): 1256–1268. doi:10.1016/j.bbamcr.2013.02.002

54. Chen W, Zhao H, Li Y (**2023**). Mitochondrial dynamics in health and disease: mechanisms and potential targets. **Signal Transduct Target Ther** 8 (1): 1–25. doi:10.1038/s41392-023-01547-9

55. Wu S, Zhou F, Zhang Z, Xing D (**2011**). Mitochondrial oxidative stress causes mitochondrial fragmentation via differential modulation of mitochondrial fission-fusion proteins. **FEBS J** 278 (6): 941–954. doi:10.1111/j.1742-4658.2011.08010.x

56. Yang L, Dong Y, Wu C, Li Y, Guo Y, Yang B, Zong X, Hamblin MR, Liu TY, Zhang Q (**2019**). Photobiomodulation preconditioning prevents cognitive impairment in a neonatal rat model of hypoxia-ischemia. **J Biophotonics** 12 (6): 201800,359. doi:10.1002/jbio.201800359

57. Yu Z, Liu N, Li Y, Xu J, Wang X (**2013**). Neuroglobin overexpression inhibits oxygen-glucose deprivation-induced mitochondrial permeability transition pore opening in primary cultured mouse cortical neurons. **Neurobiol Dis** 56: 95–103. doi:10.1016/j.nbd.2013.04.015

58. Tabak S, Schreiber-Avissar S, Beit-Yannai E (**2018**). Extracellular vesicles have variable dose-dependent effects on cultured draining cells in the eye. **J Cell Mol Med** 22 (3): 1992–2000. doi:10.1111/jcmm.13505

59. Amri F, Ghouili I, Amri M, Carrier A, Masmoudi-Kouki O (**2017**). Neuroglobin protects astroglial cells from hydrogen peroxide-induced oxidative stress and apoptotic cell death. **J Neurochem** 140 (1): 151–169. doi:10.1111/jnc.13876

60. Watanabe S, Wakasugi K (**2008**). Zebrafish Neuroglobin Is a Cell-Membrane-Penetrating Globin. **Biochemistry** 47: 5266–5270. doi:10.1021/bi800286m

61. Mendoza V, Klein D, Ichii H, Ribeiro MM, Ricordi C, Hankeln T, Burmester T, Pastori RI (**2005**). Protection of islets in culture by delivery of oxygen binding neuroglobin via protein transduction. **Transplant Proc** 37 (1): 237–240. doi:10.1016/j.transproceed.2004.12.270

62. Zhou GY, Zhou SN, Lou ZY, Zhu CS, Zheng XP, Hu XQ (**2008**). Translocation and neuroprotective properties of transactivator-of-transcription protein-transduction domain-neuroglobin fusion protein in primary cultured cortical neurons. **Biotechnol Appl Biochem** 49 (1): 25–33. doi:10.1042/BA20070061

63. Cai B, Lin Y, Xue XH, Fang L, Wang N, Wu ZY (**2011**). TAT-mediated delivery of neuroglobin protects against focal cerebral ischemia in mice. **Exp Neurol** 227 (1): 224–231. doi:10.1016/j.expneurol.2010.11.009

64. Tun S, Barathi VA, Luu CD, Lynn MN, Chan ASY (**2019**). Effects of Exogenous Neuroglobin (Ngb) on retinal inflammatory chemokines and microglia in a rat model of transient hypoxia. **Sci Rep** 9 (1): 18,799. doi:10.1038/s41598-019-55315-3

65. Sigismund S, Confalonieri S, Ciliberto A, Polo S, Scita G, Fiore PPD (**2012**). Endocytosis and Signaling: Cell Logistics Shape the Eukaryotic Cell Plan. **Physiol Rev** 92 (1): 273–366. doi:10.1152/physrev.00005.2011

66. Camblor-Perujo S, Kononenko NL (**2022**). Brain-specific functions of the endocytic machinery. **FEBS J** 289 (8): 2219–2246. doi:10.1111/febs.15897

67. Wesche J, Małecki J, Więdłocha A, Skjerpen CS, Claus P, Olsnes S (**2006**). FGF-1 and FGF-2 Require the Cytosolic Chaperone Hsp90 for Translocation into the Cytosol and the Cell Nucleus ⁎. **J Biol Chem** 281 (16): 11,405–11,412. doi:10.1074/jbc.M600477200

68. Liao HJ, Carpenter G (**2007**). Role of the Sec61 Translocon in EGF Receptor Trafficking to the Nucleus and Gene Expression. **Mol Biol Cell** 18 (3): 1064–1072. doi:10.1091/mbc.e06-09-0802

69. Giodini A (**2008**). Hsp90-mediated cytosolic refolding of exogenous proteins internalized by dendritic cells. **EMBO J** 27 (1): 201–211. doi:10.1038/sj.emboj.7601941

70. Li XH, Zhang J, Li DF, Wu W, Xie ZW, Liu Q (**2020**). Physiological and pathological insights into exosomes in the brain. **Zool Res** 41 (4): 365–372. doi:10.24272/j.issn.2095-8137.2020.043

71. O'brien K, Breyne K, Ughetto S, Laurent LC, Breakefield XO (**2020**). RNA delivery by extracellular vesicles in mammalian cells and its applications. **Nat Rev Mol Cell Biol** 21 (10): 585–606. doi:10.1038/s41580-020-0251-y

72. Kwok ZH, Wang C, Jin Y (**2021**). Extracellular Vesicle Transportation and Uptake by Recipient Cells: A Critical Process to Regulate Human Diseases. **Processes** 9 (2): 273. doi:10.3390/pr9020273

73. O'brien K, Ughetto S, Mahjoum S, Nair AV, Breakefield XO (**2022**). Uptake, functionality, and re-release of extracellular vesicle-encapsulated cargo. **Cell Rep** 39 (2): 110,651. doi:10.1016/j.celrep.2022.110651

74. Heidarzadeh M, Sokullu E, Saghati S, Karimipour M, Rahbarghazi R (**2022**). Insights into the Critical Role of Exosomes in the Brain; from Neuronal Activity to Therapeutic Effects. **Mol Neurobiol** 59 (7): 4453–4465. doi:10.1007/s12035-022-02853-z

75. Kalani A, Tyagi A, Tyagi N (**2014**). Exosomes: Mediators of Neurodegeneration, Neuroprotection and Therapeutics. **Mol Neurobiol** 49 (1): 590–600. doi:10.1007/s12035-013-8544-1

76. Zhang HG, Grizzle WE (**2014**). Exosomes: A Novel Pathway of Local and Distant Intercellular Communication that Facilitates the Growth and Metastasis of Neoplastic Lesions. **Am J Pathol** 184 (1): 28–41. doi:10.1016/j.ajpath.2013.09.027

77. Mattingly J, Li Y, Bihl JC, Wang J (**2021**). The promise of exosome applications in treating central nervous system diseases. **CNS Neurosci Ther** 27 (12): 1437–1445. doi:10.1111/cns.13743

78. Xing C, Lo EH (**2017**). Help-me signaling: Non-cell autonomous mechanisms of neuroprotection and neurorecovery. **Prog Neurobiol** 152: 181–199. doi:10.1016/j.pneurobio.2016.04.004

79. Planchon TA, Gao L, Milkie DE, Davidson MW, Galbraith JA, Galbraith CG, Betzig E (**2011**). Rapid three-dimensional isotropic imaging of living cells using Bessel beam plane illumination. **Nat Methods** 8 (5): 417–423. doi:10.1038/nmeth.1586

80. Moradi F, Fiocchetti M, Marino M, Moffatt C, Stuart JA (**2021**). Media composition and O2 levels determine effects of 17β-estradiol and selective estrogen receptor modulators on mitochondrial bioenergetics and cellular reactive oxygen species. **Am J Physiol Cell Physiol** 321 (1): C72–C81. doi:10.1152/ajpcell.00080.2021